JACS
JOURNAL OF THE AMERICAN CHEMICAL SOCIETY

ARTICLE

pubs.acs.org/JACS

DNA-Mediated Assembly of Cytochrome P450 BM3 Subdomains

Michael Erkelenz, Chi-Hsien Kuo,[†] and Christof M. Niemeyer*

TU Dortmund, Fakultät Chemie, Biologisch-Chemische Mikrostrukturtechnik, Otto-Hahn Strasse 6, D-44227 Dortmund, Germany

Supporting Information

ABSTRACT: Cytochrome P450 BM3 is a versatile enzyme, which holds great promise for applications in biocatalysis and biomedicine. We here report on the generation of a hybrid DNA−protein device based on the two subdomains of BM3, the reductase domain BMR and the porphyrin domain BMP. Both subdomains were fused genetically to the HaloTag protein, a self-labeling enzyme, allowing for the bioconjugation with chloroalkane-modified oligonucleotides. The subdomain-DNA-chimeras could be reassembled by complementary oligonucleotides, thus leading to reconstitution of the monooxygenase activity of BM3 holoenzyme, as demonstrated by conversion of the reporter substrate 12-pNCA. Arrangement of the two chimeras on a switchable DNA scaffold allowed one to control the distance between both subdomains, as indicated by the DNA-dependent activity of the holoenzyme. Furthermore, a switchable chimeric device was constructed, in which monooxygenase activity could be turned off by DNA strand displacement. This study demonstrates that P450 BM3 engineering and strategies of DNA nanotechnology can be merged to open up novel ways for the development of novel screening systems or responsive catalysts with potential applications in drug delivery.

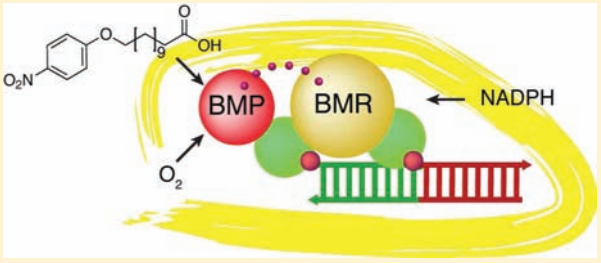

INTRODUCTION

Cytochrome P450 BM3 is one of the best studied soluble cytochrome P450 enzymes. Because it is considered and widely used as a model to study its human counterparts, many studies have focused on the structure, electron pathways, and reaction cycles catalyzed by this enzyme.[1,2] Besides the similarity to human cytochromes, the convenient heterologous expression of P450 BM3 in *E. coli* and its ability to hydroxylize inactivated C−H bonds have attracted chemists and synthetic biologists to exploit the biotechnological potential of P450 BM3. Especially protein engineers are making remarkable progress in increasing the substrate scope and tailoring the catalyzed reactions in a way that the P450 BM3 scaffold has become a most promising candidate for future applications in biotechnology.[3]

The earliest reported reactivity of P450 BM3 is the monooxygenation of the ω-2 position of fatty acids,[4] and meanwhile protein engineering has succeeded to create numerous mutants, which possess altered substrate specificity, including conversion of indole,[5] propranolol,[6] polycyclic aromatic hydrocarbons,[7] fluorogenic alkoxyresorufins,[8] terpenes,[9] as well as other components.[3] It has been demonstrated that P450 BM3 can be used in semisynthetic approaches to produce compounds of pharmaceutical interest like Artemisinin[10] or fluorine containing scaffolds.[11] In addition to creating new biocatalysts, studies aiming to simulate human metabolism with P450 BM3[12−14] or to convert the enzyme into a magnetic resonance imaging contrast agent[15] demonstrate the versatility of this enzyme system and might provide new benchmarks for P450 BM3 applications.

Native P450 BM3 is comprised of two domains, the reductase domain BMR, bearing FAD and FMN prosthetic groups, and the porphyrin domain BMP, containing the catalytic heme (protoporphyrin IX) group. P450 BM3 usually acts as a monooxygenase accepting electrons from NADPH and transferring them via FAD and FMN prosthetic groups to its heme moiety where they finally serve to reductively cleave molecular oxygen and use one oxygen atom for substrate hydroxylation (Figure 1).[1] Because the detailed mechanism of electron transfer on the atomic level is still the subject of current research,[16−18] crucial questions include influences of the relative distances of the redox centers as well as the contact interface between BMP and BMR domains. It has been demonstrated that BMP and BMR domains can be expressed separately and that the NADPH-dependent fatty acid hydroxylase function of the holoenzyme can be reconstituted by using one of the domains in large excess.[19,20] While this observation indicated that intermolecular electron transfer can occur between the BMP and BMR domains, the low activity of only about 5% of that of the wild-type holoenzyme suggested that physical contact plays an important role for electron transfer. It is also of interest that both domains constitute independent catalytic entities. Some variants of BMP, in particular mutant F87A,[21] can hydroxylate substrates via the so-called peroxide shunt pathway, in which H_2O_2 is used instead of NADPH, thereby rendering BMR dispensable.[22] On the other hand, BMR can catalyze the reduction of various compounds with NADPH, such as cytochrome C, in a stand-alone reaction.[4]

Received: June 6, 2011
Published: September 15, 2011

The enormous relevance of P450 BM3 for biotechnological applications and the system's modularity led us to the idea that BMP and BMR might represent ideal candidates for design and construction of an artificial allosterically tunable hybrid enzyme, in which variation of the relative spatial orientation of the two functional domains would not only allow for fundamental mechanistic studies of electron transfer processes in multi domain proteins but also for applications in biotechnology.

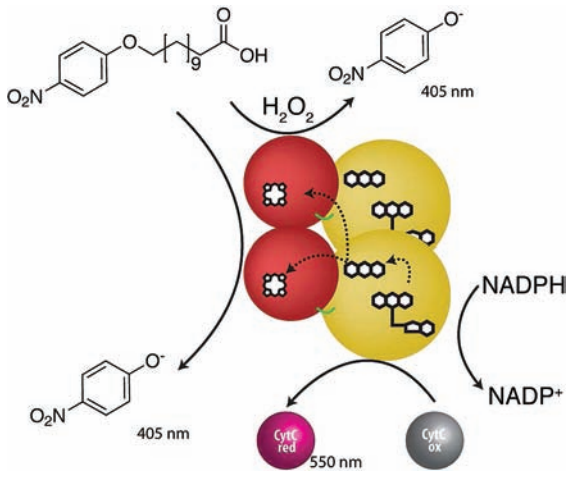

Figure 1. P450 BM3-catalyzed reactions and proposed electron pathways in putative dimer of BM3 holoenzymes. In the NADPH-dependent conversion of 12-pNCA, the electrons are transferred from NADPH via FAD to FMN of the BMR domain (yellow spheres) of monomer 1 and subsquently to the heme group of BMP (red sphere) of monomer 2. Note that BMP can hydroxylate 12-pNCA in the absence of BMR and NADPH using H_2O_2 in the peroxide shunt pathway. Note also that electrons from NADPH can be transferred to cytochrome C, thus giving rise to monitor activity of the isolated BMR domain photometrically.

A potential approach to generate conformationally switchable multifunctional protein entities is based on the combination of structural DNA nanotechnology[23−25] with semisynthetic DNA−protein conjugates, which enables complementation of protein function with the specific addressability of synthetic DNA oligonucleotides.[26] This approach has already been used to trigger activity of single domain proteins, such as allosteric enzyme activation,[27,28] reconstitution of apoenzymes,[29,30] complementation of split fluorescent proteins[31] and enzymes,[32] or the cascading of individual consecutive operating enzymes.[30,33−35] While these studies primarily aimed toward establishment of biosensors, no work has yet been reported on the use of DNA scaffolds for systematic variation of spatial configurations of multi domain enzymes, such as BM3. We here report on the assembly of BMP and BMR domains and the allosteric regulation of functional holoenzyme based on DNA hybridization.

EXPERIMENTAL SECTION

A detailed description of cloning and heterologous expression of BMR and BMP fusion proteins, 12-pNCA synthesis, oligonucleotide sequences, synthesis and characterization of DNA−protein conjugates, enzyme assays and determination of hybridization kinetics, as well as model estimations on the spatial configuration of DNA-linked BM3 subdomains is given in the Supporting Information.

RESULTS AND DISCUSSION

To investigate the possibility of linking the monooxygenase reaction of P450 BM3 to a DNA-dependent control mechanism, we used the well-known variant P450 BM3 F87A,[5,36−38] which catalyzes the hydroxylation of the reporter substrate *p*-nitrophenoxycarboxylic acid (12-pNCA).[37] Variant P450 BM3 F87A not only shows enhanced activity with 12-pNCA substrates as

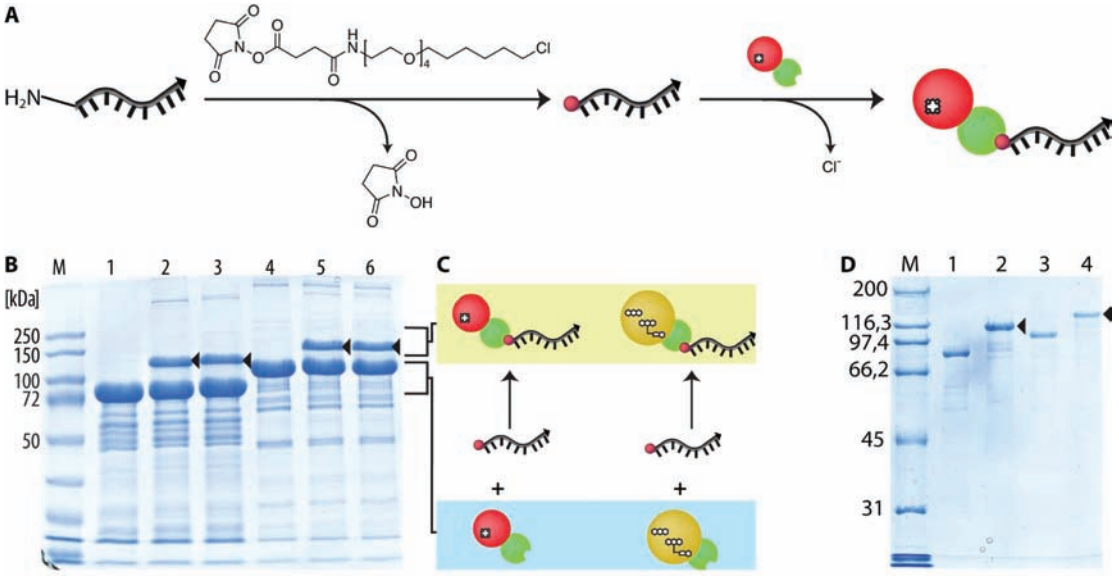

Figure 2. Schematic representation (A) and SDS-PAGE analysis (B) of protein−DNA conjugation. These are a Coomassie-stained gels. Unreacted BMP-F87A-Halo and BMR-Halo are in shown lanes 1 and 4, respectively. Crude reaction mixtures are shown obtained from conjugation of BMP-F87A-Halo + chlorohexane-aF9 (lane 2), BMP-F87A-Halo + chlorohexane-acF9 (lane 3), BMR-Halo + chlorohexane-aF9 (lane 5), and BMR-Halo + chlorohexane-acF9 (lane 6). Black triangles indicate the conjugate bands. The presence of DNA in the slower migrating bands of the conjugates was confirmed by SybrGold staining (Figure S2, Supporting Information). (C) Schematic representation of fusion proteins and their DNA conjugates. (D) SDS-PAGE analysis of conjugates purified by anion-exchange chromatography: lane 1, BMP-Halo; lane 2, BMP-Halo-aF9; lane 3, BMR-Halo; lane 4, BMR-Halo-acF9.

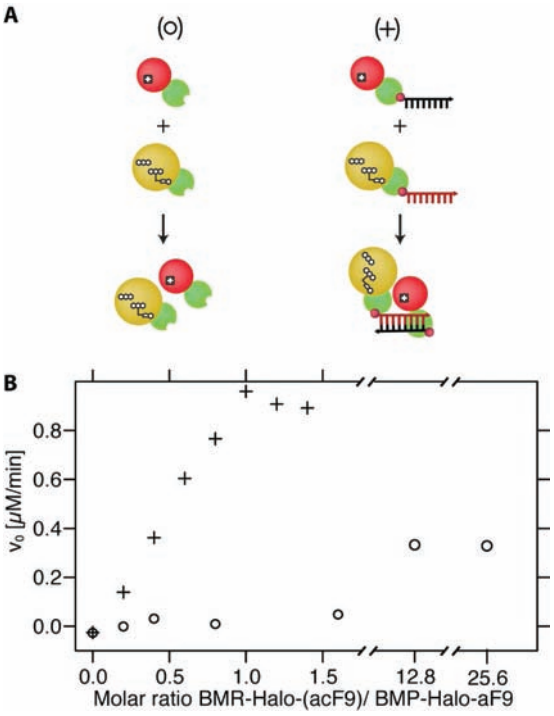

Figure 3. Establishment of DNA-based reassembly of BM3 holoenzyme by titration of BMP-Halo-aF9 with complementary BMR-Halo-acF9. (A) Schematic representation of the conducted experiments. (B) Plot of the initial rate of 12-pNCA conversion (v_0) versus the relative molar ratio of BMP to BMR domains. Shown are two experiments in which BMR-Halo was titrated with increasing amounts of BMP-Halo (○) and DNA−protein conjugates BMP-Halo-aF9 with increasing amounts of BMR-Halo-acF9 (+).

compared to the wild-type, but it also catalyzes hydroxylation of fatty acids by employment of the so-called peroxide shunt pathway, that is, that H_2O_2 is used as the cosubstrate instead of NADPH.[21] In the presence of the native cofactor NADPH, electrons are transferred from NADPH to the FAD/FMN prosthetic groups of BMR to the heme group of BMP where they are used to reduce molecular oxygen, thereby forming compound II, which finally enables substrate oxidation (Figure 1). Although the exact electron pathway is still the subject of current research, it has recently been suggested that a dimer of holoenzymes constitutes the active form of P450 BM3.[16−18] According to this hypothesis, the electrons are transferred in this dimer from NADPH via FAD to the FMN group of monomer 1 and subsquently to the heme group of the BMP domain of monomer 2 (Figure 1). As described above, the modular BMR/BMP system offers the advantage that enzymatic activity of reconstituted BM3 holenenzyme can be assayed by NADPH-dependent 12-pNCA conversion, while activity of the BMR and BMP domain alone can be monitored by the reduction of cytochrome C,[4] which shows increased absorption at 550 nm in its reduced state,[39] or the H_2O_2-dependent 12-pNCA conversion, respectively (Figure 1).

To facilitate site-selective conjugation of BMR and BMP with DNA oligonucleotides under mild conditions, we used a previously reported method,[40] which is based on self-labeling fusion proteins, such as the HaloTag.[41] The encoding DNA of the two subdomains BMP-F87A and BMR was cloned into pEXP-n9 expression plasmids to enable for the C-terminal fusion with a HaloTag domain (Figure S1, Supporting Information). After expression and purification, the recombinant proteins BMP-F87A-Halo and BMR-Halo were both conjugated with single-stranded oligonucleotides bearing a chlorohexane substituent, which is the suicide substrate for the HaloTag and establishes a permanent covalent bond between the DNA oligonucleotide and the protein (Figure 2A).

For an initial test of function, we chose two oligonucleotides, which are complementary to each other, termed as aF9 and acF9, for the conjugation with BMP-Halo and BMR-Halo, respectively. The formation of the expected DNA−protein conjugates BMP-Halo-aF9 and BMR-Halo-acF9 was confirmed by SDS-PAGE analysis (Figure 2B). Crude reaction mixtures were purified to homogeneity by anion exchange chromatography (Figure 2D and Figure S3, Supporting Information). It should be noted that chromatographic separation of BMP-Halo- and BMR-Halo-DNA conjugates from the unreacted proteins was hampered by a relatively high tendency of aggregation, in particular for the BMR-Halo protein, leading to partial coelution of the conjugated and unconjugated protein. The tendency of dimer formation has previously been reported for P450 BM3.[42] The purified conjugates were quantified by the Bradford assay, and extinction coefficients at 260 and 280 nm were determined (Table S4, Supporting Information). A 260/280 ratio of greater than 1 was observed, which is indicative for DNA−protein conjugates.[43] The same synthetic method was used to generate BMP-Halo- and BMR-Halo-DNA conjugates from a number of oligonucleotides with different sequences (Table S2, Supporting Information). Yields of purified conjugates were typically about 30% with respect to the amount of chlorohexane-derivatized oligonucleotide used in the synthesis. The ready applicability and efficiency of BMP- and BMR-DNA conjugate syntheses carried out in this study underlined the versatility and power of the recently developed HaloTag-based coupling strategy.[40] It should be noted, however, that the fusion with the HaloTag domain led to reduced enzyme activity, as determined by Michaelis−Menten kinetic analysis of BMP- and BMR-Halo fusion proteins and their DNA conjugates. In particular, k_{cat} values were significantly lower, while K_M values remained almost unchanged, as compared to wild-type BM3 and native F87A BM3 (Table S1, Supporting Information). To omit bulky connectors and to elucidate the influence of sterical factors, further developments may include more direct chemical coupling systems, such as alkyne−azide cycloaddition or other bioorthogonal linking chemistries.[26]

To investigate whether the cloned domains can be reassembled to the functional BM3 holoenzyme, we initially carried out titration experiments (Figure 3). To this end, initial controls were conducted in which the recombinant BMP-Halo was mixed with increasing amounts of BMR-Halo. As indicated by the circular data points in Figure 3, a large excess of BMR-Halo (>10 mol equiv) was necessary to initiate assembly of the two domains, as indicated by 12-pNCA conversion. In strong contrast, titration of BMP-Halo-aF9 with increasing amounts of BMR-Halo-acF9 revealed that active holoenzyme is formed even in the case of substoichiometric amounts of BMR-Halo-acF9 (<1 mol equiv, crossed data points in Figure 3). Maximum activity was obtained when the two DNA-conjugated domains were present in equimolar amounts and further increase of BMR-Halo-acF9 did not lead to significant changes in the rate of 12-pNCA conversion. We also confirmed that complementarity of the two protein tethered oligonucleotides is necessary for

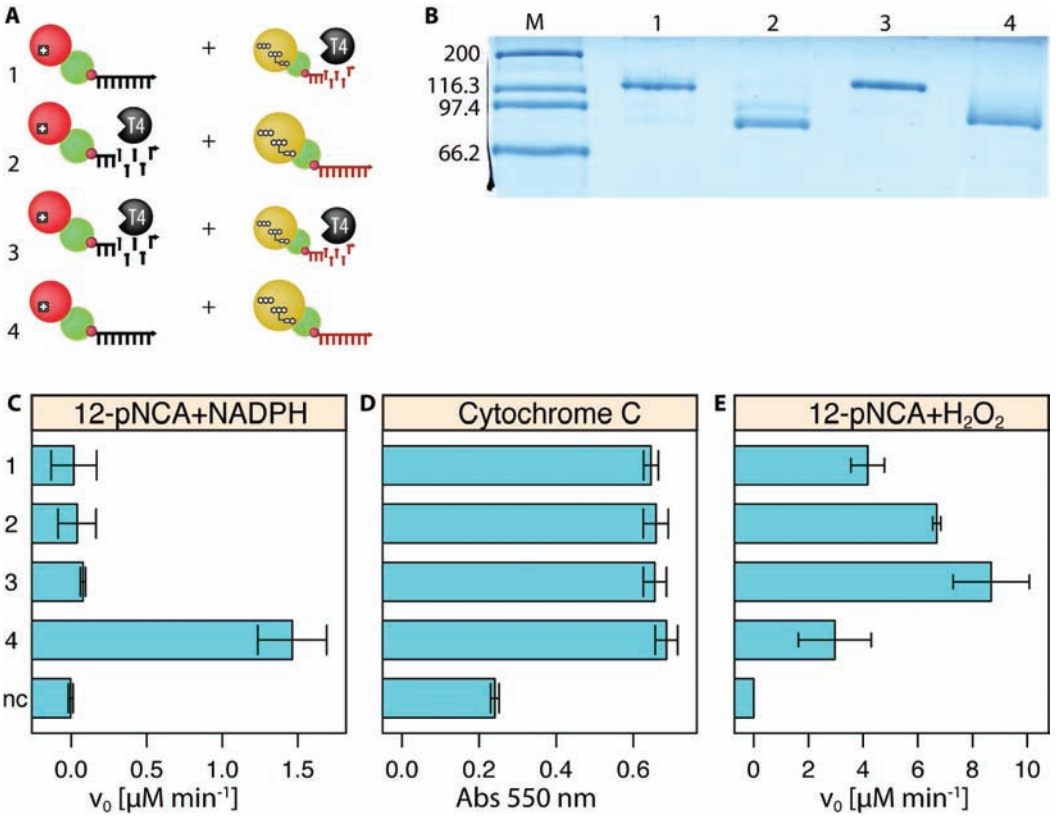

Figure 4. Digestion and activity analysis of DNA−protein conjugates. The oligonucleotide moiety of BMP-Halo-aF9 or BMR-Halo-acF9 was digested with T4-Polymerase. Subsequently, all possible combinations of undigested and digested DNA−protein conjugates were prepared, and the enzymatic activity of these mixtures was tested, as schematically depicted in (A). (B) SDS-PAGE analysis of T4-polymerase digestion. M, broad range marker; lane 1, BMP-Halo-aF9; lane 2, digested BMP-Halo-aF9; lane 3, BMR-Halo-acF9; lane 4, digested BMR-Halo-acF9. (C) The activity of digested/undigested DNA−protein conjugate combinations depicted in (A) was assayed with NADPH/12-pNCA to determine which combination is capable of reassembling functional holoenzyme. Mixtures were also analyzed with NADPH/cytochrome C to independently determine BMR activity (D) or with H_2O_2/12-pNCA to independently determine BMP activity (E). Error bars indicate deviations obtained in three independent experiments. NC denotes activity measured in a negative control where no protein species were present.

reassembly of functional BM3 holoenzyme. As discussed below in the context of Figure 6, equimolar mixtures of the two non-complementary DNA−protein conjugates BMP-Halo-aF9 and BMR-Halo-aF1 did not show any conversion of 12-pNCA. These results clearly indicate that reassembly of functional BM3 holoenzyme is indeed mediated by and dependent on hybridization of the complementary DNA oligonucleotides.

To analyze whether and how conjugation of DNA oligonucleotides affects the activity of the two isolated domains, we digested the oligonucleotide moiety of BMP-Halo-aF9 and BMR-Halo-acF9 with T4-Polymerase. This enzyme has an exonuclease activity in the absence of dNTPs.[44] Successful removal of the conjugated oligonucleotide was confirmed by SDS-PAGE analysis (Figure 4B). The digested samples were mixed with equimolar amounts of undigested conjugates to prepare all possible combinations of binary mixtures of digested/undigested BMR and BMP domains. These mixtures were then analyzed with NADPH/12-pNCA to prove that reassemby of functional holoenzyme is possible only in the case of two undigested domains (entry 4 in Figure 4C). However, velocity rates ($v_0 \approx 1.5\ \mu$M/min) were slightly higher than those observed in the analogous experiment in Figure 3 ($v_0 \approx 0.9\ \mu$M/min). We attribute this increase in activity to changed buffer conditions, likely DTT and/or Mg^{2+}, which are components of the T4-polymerase digestion buffer (see experimental section in the Supporting Information). Moreover, activity of BMR in the mixtures was confirmed by cytochrome C reduction in the presence of NADPH cofactor (Figure 4D). As expected, all samples revealed almost identical activity in cytochrome C reduction, thereby indicating that neither DNA conjugation nor T4-polymerase digestion interfered with the activity of the reductase domain. Taking advantage of the peroxide shunt pathway, the mixtures were also assayed with H_2O_2/12-pNCA to independently determine BMP activity (Figure 4E). All mixture showed conversion of 12-pNCA, thus indicating intactness of the BMP domains. However, notable differences in the reaction rates were observed. The samples 2 and 3 in which BMP conjugates were digested showed a higher activity than those containing intact BMP conjugates (samples 1 and 4, in Figure 4E). This suggests that the conjugated oligonucleotide slightly reduces the activity of BMP. Interestingly, the activity of BMP conjugates seemed to be dependent on the state of the BMR conjugates. We observed that both free and DNA-conjugated BMP-Halo showed slightly higher activity when the BMR conjugates were digested: Comparison of either samples 3 and 2, or else samples 1 and 4, containing digested and undigested BMR, respectively, reveal a slightly higher activity in samples containing digested BMR. Although the increase is

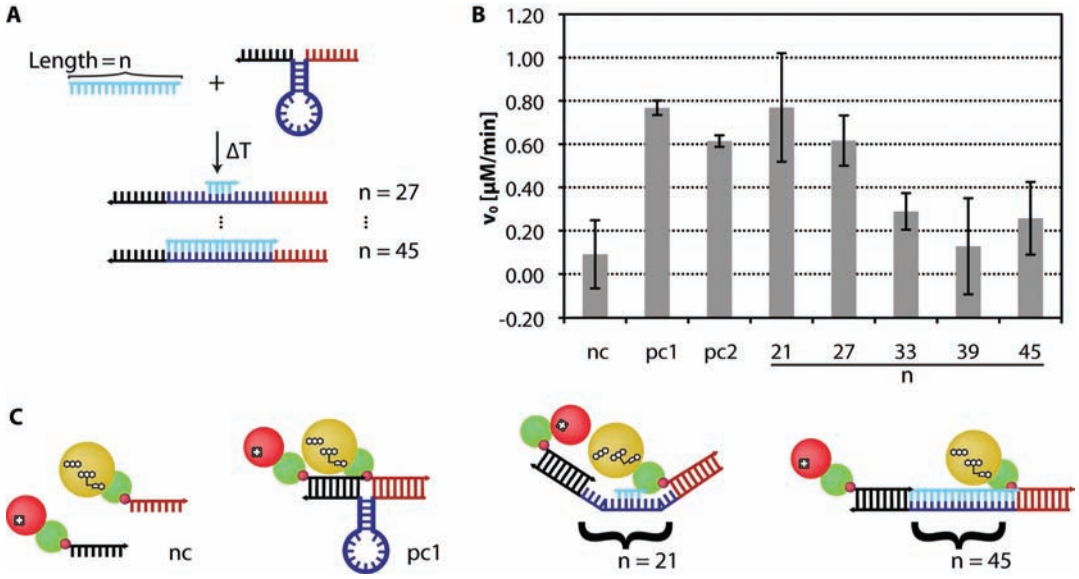

Figure 5. Looped DNA scaffold as the template for BM3 reassembly. (A) Schematic drawing of the scaffold containing two addresses (black and red portions, complementary to BMP-Halo-aF9 and BMR-Halo-aF1) connected by a stem loop (dark blue). The stem loop can be destabilized by hybridization with complementary effector oligonucleotides (light blue) of different numbers of nucleotides (n). (B) Various scaffolds, preformed from the stem loop and effectors, were used for assembly of BM3 holoenzyme by hybridization with BMP-Halo-aF9 and BMR-Halo-aF1. The height of the bars represents the initial rate of 12-pNCA conversion measured. Data in nc denotes a negative control lacking a DNA scaffold; pc1 is a positive control using the stem loop in the absence of effector oligomers; and pc2 is a positive control as in pc1, where a noncomplementary 51 nt effector was added. (C) Schematic representation of putative configurations of selected samples.

close to average deviations, it might suggest a mechanistic effect, such as a conformational change of BMP induced by BMR, which can occur more effectively in the absence of conjugated oligonucleotide.

Because the above results clearly indicated successful DNA conjugation of BMR and BMP domains as well as DNA-based reassembly of functional BM3 holoenzyme, we attempted to build more complex DNA−protein architecture. To this end, a DNA scaffold was designed in which a stem-loop structure was inserted between two address sequences, cF1 and cF9, complementary to conjugates BMR-Halo-aF1 and BMP-Halo-aF9, respectively (Figure 5). The stem-loop substructure contained a 11 bp double-stranded stem and an open 23 nucleotide (nt) loop. We reasoned that the stem loop should be destabilized upon hybridization with complementary effector oligonucleotides of different length, thereby leading to altered distances of hybridized protein conjugates, and consequently to a change in activity of reconstituted holoenzyme. To test this hypothesis, various scaffolds were preformed from the stem loop and effectors (PME oligomers in Table S2), and the resulting duplex structures were used for assembly of BM3 holoenzyme by hybridization with BMP-Halo-aF9 and BMR-Halo-aF1. Catalytic activity of reconstituted holoenzyme was measured by determining the initial rate of 12-pNCA conversion in the presence of NADPH (Figure 5B). A negative control lacking the DNA scaffold revealed no activity, as expected. Positive controls, in which the stem-loop oligomer was used in the absence or the presence of a noncomplementary effector (pc1 or pc2, respectively, in Figure 5B), showed a high activity. Because initial velocity rates ($v_0 \approx 0.8\ \mu$M/min) were similar to that obtained for the binary superstructures described above ($v_0 \approx 0.9\ \mu$M/min, Figure 3), one may conclude that the undisturbed stem-loop scaffold enables similar effective contacts between the BMR and BMP domain.

In contrast, scaffolds containing partial duplex regions led to decreased activity of the holoenzyme superstructures. Short effectors (n = 21 or 27 nt) had only little influence on holoenzyme activity, while longer effectors (n = 33, 39, or 45 nt) led to significant reduction in enzyme activity. As determined by Förster resonance energy transfer (FRET) measurements (Figure S4, Supporting Information), hybridization with the 39 or 45 nt effectors opens the stem-loop, while shorter effectors (n = 21, 27, or 33 nt) are not capable of stem-loop opening in the absence of proteins. In conjunction with geometric model calculations to estimate spatial dimensions of DNA-assembled constructs (Figure S5, Supporting Information), the observation that the 39 nt and 45 nt effectors almost completely shut down holoenzyme activity (Figure 5B) suggests that the linearized stem loop−effector duplex displays sufficient rigidity to effectively separate BMR and BMP domains. Even though the duplex can bend and rotate at sites where the dsDNA backbone is nicked or incomplete, a linear double helix seems favored, presumably due to stacking interactions and electrostatic repulsion. Interestingly, the 33 nt effector clearly induced a decrease in holoenzyme activity (Figure 5B), while it was not able to open the stem-loop in the absence of proteins (Figure S4B). This observation suggests that protein conjugation weakens the stability of the adjacent stem loop. To sum, the results obtained with this initial system clearly demonstrate that designed DNA scaffolds can be used to adjust physical contact of two interacting protein domains and thus tune the rate of electron transfer.

We also tested whether the BMR and BMP domains in active stem-loop DNA−protein superstructures can be pulled apart from each other by hybridization with effector oligomers. For example, the undisturbed stem-loop superstructure pc1 (Figure 5C) was incubated with the 45 nt effector during 12-pNCA conversion. Because no clear decrease in activity could be

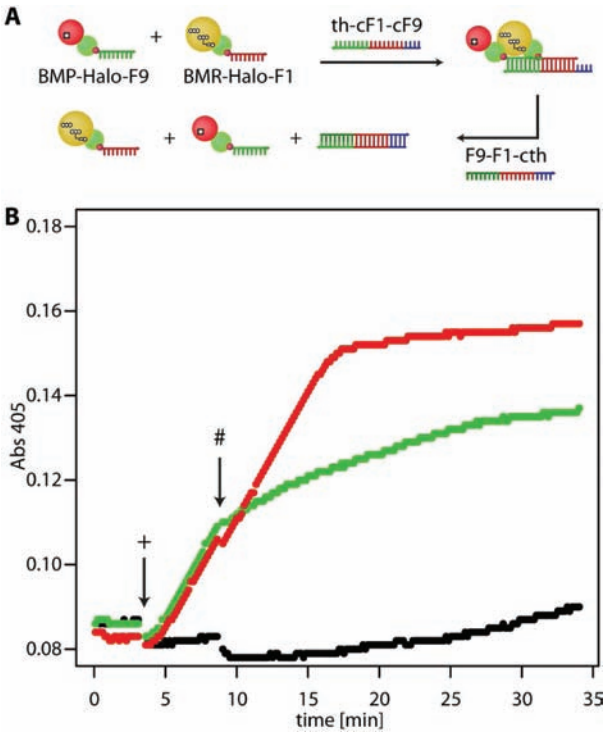

Figure 6. Reversible assembly of BM3 domains. (A) Schematic drawing of the DNA-mediated assembly and disassembly of BM3 holoenzyme by strand displacement. Template th-cF1-cF9 can bind the two BM3 domains BMP-Halo-aF9 and BMR-Halo-aF1 with its red and green portions, respectively. The blue colored single-stranded 10 nt toehold is used to initiate strand displacement by hybridization with oligomer F9-F1-cth, which is fully complementary to template th-cF1-cF9. The formation of the duplex leads to release of BMP-Halo-aF9 and BMP-Halo-aF1. (B) Plot of 12-pNCA conversion measured by absorbance at 405 nm versus time. To three identical samples containing BMP-Halo-aF9, BMP-Halo-aF1, NADPH, and 12-pNCA was added either template th-cF1-cF9 (red and green curves) or a noncomplementary oligonucleotide (black curve) at time point (+). Note that addition of template leads to immediate formation of active enzyme. At time point (#), either stopper oligomer F9-F1-cth (green curve) or a noncomplementary control oligonucleotide (red and black curves) was added. Note that stopper F9-F1-cth led to a decrease in 12-pNCA conversion (green curve), while the noncomplementary control strand did not affect holoenzyme activity (red curve).

observed, we analyzed the stem-loop system in the absence of proteins by measuring the kinetics of hybridization with the longest effector using a FRET approach (Figure S6, Supporting Information). Although this model reaction indicated switchability of our stem-loop system, we observed very slow hybridization kinetics, which is in good agreement with a previous study on DNA hairpins.[45] It was therefore evident that the loop opening did not proceed sufficiently fast to enable measurement of changes in the enzymatic conversion of pNCA.

To circumvent the obstacles of the above-described stem-loop system, we explored another DNA design for demonstration of reversible domain assembly. To this end, the linear single-stranded template th-cF1-cF9 was chosen (Figure 6), which contains the two binding sites for BMR-Halo-aF1 and BMP-Halo-aF9 in addition to a 10 nt toehold sequence. The toehold initiates hybridization with stopper oligomer F9-F1-cth, which is fully complementary to template th-cF1-cF9. This process leads to complete strand displacement and thus release of BMP-Halo-aF9 and BMP-Halo-aF1 from the template. Because of the absence of secondary structures within the th-cF1-cF9 and F9-F1-ct oligomers, the system was expected to react faster than the stem-loop system. Second-order rate constants of $10^5-10^6\ M^{-1}\ s^{-1}$ have been reported for strand displacement reactions with linear sequences.[46] On the basis of these constants, the strand displacement system should exhibit reaction time half-lives of 2−20 s, at initial reactant concentrations of 0.5 μM (Figure S7, Supporting Information). Thus, strand displacement should lead to detectable signals within the time scale of less than 30 min. This estimation was experimentally confirmed by analysis of the strand displacement of the th-cF1-cF9/F9-F1-ct oligomers using a FRET approach (Figure S6). Indeed, displacement showed a half life of only a few seconds. We then applied this oligonucelotide system for assembly and disassembly of the BMP- and BMR-DNA conjugates. It is clearly evident from the green and red curves in Figure 6 that addition of template th-cF1-cF9 to a mixture of BMR-Halo-aF1 and BMP-Halo-aF9 led to immediate formation of functional holoenzyme. After about 10 min, stopper oligomer F9-F1-cth was added. This led to a marked effect on the reaction rate, which was not observed in a control reaction where the noncomplementary oligomer PME 38 was added (green vs red curve in Figure 6). Addition of the stopper immediately decreased the slope of reaction rate (green curve), while the noncomplementary control oligonucleotide did not affect holoenzyme activity of reassembled BMR-BMP (red curve). However, no abrupt stopping occurred upon addition of the complementary stopper (green curve), presumably due to a comparably slow dissociation kinetics and/or attractive interactions of BMP and BMR domains. Nonetheless, these results clearly indicate the functionality of assembly and disassembly of BM3 holoenzyme by means of designed DNA templates.

CONCLUSIONS

We here demonstrated that DNA-based assembly of the two subdomains of BMP and BMR can be harnessed to create a tunable monooxygenase system. BMP and BMR domains conjugated with synthetic oligonucleotides can be reversibly assembled and disassembled by aid of appropriate DNA scaffolds. DNA-based protein assembly has already been used to create biocatalytic cascades of consecutively working enzymes, such as glucose oxidase (GOx) and horseradish peroxidase (HRP).[30,33−35] This approach to functional coupling of enzymes aims at improving the reaction efficiency by limiting the diffusion distance between catalytic centers for the intermediate reactant, such as H_2O_2 in the case of the GOx/HRP system. In contrast to this approach, we here describe a system that enables control of enzyme activity by a DNA-dependent mechanism. To the best of our knowledge, this is the first study that demonstrates the directional incorporation of two delicate protein domains in functional DNA scaffolds to enable control of enzymatic activity by tunable approximation of two subdomains. Resulting changes in distance between the redox centers embedded in the BMP and BMR domains in turn regulate efficiency of electron transfer, and thus enzymatic activity of the reconstituted holoenzyme. It should be noted that more rigid scaffolds, such as DNA double-crossover tiles or origami superstructures, may serve even better as molecular pegboard and ruler to study distance dependency of transport processes in reassembled multidomain proteins. However, methods to synthesize such

DNA−protein superstructures on a preparative scale are not yet available.

One important technical feature of the here reported system stems from the fact that both domains not only display a specific activity when brought together but that the domains can be interrogated independently by convenient analytical assays. This aspect clearly exceeds the concept of split enzymes, where the separated components have no stand-alone activity,[32] and it will be of great importance for future development of advanced BM3-based systems. It has already been emphasized that the BMP domain can be adopted to the specific conversion of a broad range of substrates by directed evolution,[3] and, likewise, engineering of BMR enables control over the cofactor, which, for instance, can be switched from NADPH to NADH.[47] Hence, immediate perspectives of the modular BMR/BMR assembly system arise from the fact that it can be used for ready exploration of combinatorial assemblies of different P450 and reductase domains to find suitable combinations. This approach will significantly reduce the amount of cloning. Moreover, the control of spatial configuration of the two domains by DNA scaffolds adds an additional degree of freedom, because nucleic acid hybridization is highly specific and its kinetics can be easily controlled.[46] One may thus foresee long-term applications in which switchable DNA-BMP/BMR constructs are used for drug delivery. For instance, constructs could be designed to be triggered by micro RNAs, which are endogeneously expressed during development and disease.[48] Binding to nucleic acid targets could switch on the construct's activity, thereby enabling localized enzymatic activation of prodrugs. In view of these perspectives, we anticipate that the concept demonstrated here could open up ways for the development of novel screening systems or responsive biocatalysts for therapeutic applications.

■ ASSOCIATED CONTENT

Supporting Information. A detailed description of cloning and heterologous expression of BMR and BMP fusion proteins, 12-pNCA synthesis, oligonucleotide sequences, synthesis and characterization of DNA−protein conjugates, enzyme assays and determination of hybridization kinetics, as well as model estimations on the spatial configuration of DNA-linked BM3 subdomains. This material is available free of charge via the Internet at http://pubs.acs.org.

■ AUTHOR INFORMATION

Corresponding Author

christof.niemeyer@tu-dortmund.de

Present Addresses

[†]Institute of Chemistry, Academia Sinica, 128 Academia Road Sec. 2, Nankang, Taipei 11529, Taiwan.

■ ACKNOWLEDGMENT

We thank Andreas Arndt for assistance in protein expression, Barbara Sacca for help in the design of DNA nanostructures, Rebecca Meyer for assistance in the purification and modification of oligonucleotides, and Marc Skoupi and Katja Straub for contributions in cloning. This work was supported in part by the Deutsche Forschungsgemeinschaft (DFG) through project NI 399/10, the project SMD in the course of FP7-NMP-2008-SMALL-2, founded by the European Comission, and the Zentrum für Angewandte Chemische Genomik (ZACG). C.-H.K. acknowledges support through the International Max-Planck Research School in Chemical Biology, Dortmund, and a student fellowship from Deutscher Akademischer Austauschdienst (DAAD).

■ REFERENCES

(1) Munro, A. W.; Daff, S.; Coggins, J. R.; Lindsay, J. G.; Chapman, S. K. *Eur. J. Biochem.* **1996**, *239*, 403–409.
(2) Warman, A. J.; Roitel, O.; Neeli, R.; Girvan, H. M.; Seward, H. E.; Murray, S. A.; McLean, K. J.; Joyce, M. G.; Toogood, H.; Holt, R. A.; Leys, D.; Scrutton, N. S.; Munro, A. W. *Biochem. Soc. Trans.* **2005**, *33*, 747–753.
(3) Jung, S. T.; Lauchli, R.; Arnold, F. H. *Curr. Opin. Biotechnol.* **2011**, *22*, in press; DOI 10.1016/j.copbio.2011.02.008.
(4) Narhi, L. O.; Fulco, A. J. *J. Biol. Chem.* **1986**, *261*, 7160–7169.
(5) Li, Q. S.; Schwaneberg, U.; Fischer, P.; Schmid, R. D. *Chemistry* **2000**, *6*, 1531–1536.
(6) Otey, C. R.; Bandara, G.; Lalonde, J.; Takahashi, K.; Arnold, F. H. *Biotechnol. Bioeng.* **2006**, *93*, 494–499.
(7) Carmichael, A. B.; Wong, L. L. *Eur. J. Biochem.* **2001**, *268*, 3117–3125.
(8) Lussenburg, B. M.; Babel, L. C.; Vermeulen, N. P.; Commandeur, J. N. *Anal. Biochem.* **2005**, *341*, 148–155.
(9) Seifert, A.; Vomund, S.; Grohmann, K.; Kriening, S.; Urlacher, V. B.; Laschat, S.; Pleiss, J. *ChemBioChem* **2009**, *10*, 853–861.
(10) Dietrich, J. A.; Yoshikuni, Y.; Fisher, K. J.; Woolard, F. X.; Ockey, D.; McPhee, D. J.; Renninger, N. S.; Chang, M. C.; Baker, D.; Keasling, J. D. *ACS Chem. Biol.* **2009**, *4*, 261–267.
(11) Rentmeister, A.; Arnold, F. H.; Fasan, R. *Nat. Chem. Biol.* **2009**, *5*, 26–28.
(12) Reinen, J.; Kalma, L. L.; Begheijn, S.; Heus, F.; Commandeur, J. N.; Vermeulen, N. P. *Xenobiotica* **2011**, *41*, 59–70.
(13) Sawayama, A. M.; Chen, M. M.; Kulanthaivel, P.; Kuo, M. S.; Hemmerle, H.; Arnold, F. H. *Chemistry* **2009**, *15*, 11723–11729.
(14) van Leeuwen, J. S.; Vredenburg, G.; Dragovic, S.; Tjong, T. F.; Vos, J. C.; Vermeulen, N. P. *Toxicol. Lett.* **2011**, *200*, 162–168.
(15) Shapiro, M. G.; Westmeyer, G. G.; Romero, P. A.; Szablowski, J. O.; Kuster, B.; Shah, A.; Otey, C. R.; Langer, R.; Arnold, F. H.; Jasanoff, A. *Nat. Biotechnol.* **2010**, *28*, 264–270.
(16) Neeli, R.; Girvan, H. M.; Lawrence, A.; Warren, M. J.; Leys, D.; Scrutton, N. S.; Munro, A. W. *FEBS Lett.* **2005**, *579*, 5582–5588.
(17) Kitazume, T.; Haines, D. C.; Estabrook, R. W.; Chen, B.; Peterson, J. A. *Biochemistry* **2007**, *46*, 11892–11901.
(18) Girvan, H. M.; Dunford, A. J.; Neeli, R.; Ekanem, I. S.; Waltham, T. N.; Joyce, M. G.; Leys, D.; Curtis, R. A.; Williams, P.; Fisher, K.; Voice, M. W.; Munro, A. W. *Arch. Biochem. Biophys.* **2010**, *507*, 75–85.
(19) Boddupalli, S. S.; Oster, T.; Estabrook, R. W.; Peterson, J. A. *J. Biol. Chem.* **1992**, *267*, 10375–10380.
(20) Sevrioukova, I.; Truan, G.; Peterson, J. A. *Arch. Biochem. Biophys.* **1997**, *340*, 231–238.
(21) Li, Q. S.; Ogawa, J.; Shimizu, S. *Biochem. Biophys. Res. Commun.* **2001**, *280*, 1258–1261.
(22) Ortiz de Montellano, P. R.; De Voss, J. J. *Nat. Prod. Rep.* **2002**, *19*, 477–493.
(23) Seeman, N. C. *Nature* **2003**, *421*, 427–431.
(24) Simmel, F. C.; Dittmer, W. U. *Small* **2005**, *1*, 284–299.
(25) Lin, C.; Liu, Y.; Yan, H. *Biochemistry* **2009**, *48*, 1663–1674.
(26) Niemeyer, C. M. *Angew. Chem., Int. Ed.* **2010**, *49*, 1200–1216.
(27) Gianneschi, N. C.; Ghadiri, M. R. *Angew. Chem., Int. Ed.* **2007**, *46*, 3955–3958.
(28) Saghatelian, A.; Guckian, K. M.; Thayer, D. A.; Ghadiri, M. R. *J. Am. Chem. Soc.* **2003**, *125*, 344–345.
(29) Fruk, L.; Niemeyer, C. M. *Angew. Chem., Int. Ed.* **2005**, *44*, 2603–2606.

(30) Wilner, O. I.; Weizmann, Y.; Gill, R.; Lioubashevski, O.; Freeman, R.; Willner, I. *Nat. Nanotechnol.* **2009**, *4*, 249–254.
(31) Takeda, S.; Tsukiji, S.; Ueda, H.; Nagamune, T. *Org. Biomol. Chem.* **2008**, *6*, 2187–2194.
(32) Oltra, N. S.; Bos, J.; Roelfes, G. *ChemBioChem* **2010**, *11*, 2255–2258.
(33) Niemeyer, C. M.; Koehler, J.; Wuerdemann, C. *ChemBioChem* **2002**, *3*, 242–245.
(34) Müller, J.; Niemeyer, C. M. *Biochem. Biophys. Res. Commun.* **2008**, *377*, 62–67.
(35) Wilner, O. I.; Shimron, S.; Weizmann, Y.; Wang, Z. G.; Willner, I. *Nano Lett.* **2009**, *9*, 2040–2043.
(36) Oliver, C. F.; Modi, S.; Sutcliffe, M. J.; Primrose, W. U.; Lian, L. Y.; Roberts, G. C. *Biochemistry* **1997**, *36*, 1567–1572.
(37) Schwaneberg, U.; Schmidt-Dannert, C.; Schmitt, J.; Schmid, R. D. *Anal. Biochem.* **1999**, *269*, 359–366.
(38) Li, Q. S.; Schwaneberg, U.; Fischer, M.; Schmitt, J.; Pleiss, J.; Lutz-Wahl, S.; Schmid, R. D. *Biochim. Biophys. Acta* **2001**, *1545*, 114–121.
(39) Mahler, H. R. DPNH cytochrome c reductase (animal). *Methods in Enzymology*, 2nd ed.; Academic Press: New York, 1955; pp 688−693.
(40) Sacca, B.; Meyer, R.; Erkelenz, M.; Kiko, K.; Arndt, A.; Schroeder, H.; Rabe, K. S.; Niemeyer, C. M. *Angew. Chem., Int. Ed.* **2010**, *49*, 9378–9383.
(41) Los, G. V.; Wood, K. *Methods Mol. Biol.* **2007**, *356*, 195–208.
(42) Black, S. D.; Martin, S. T. *Biochemistry* **1994**, *33*, 12056–12062.
(43) Niemeyer, C. M.; Sano, T.; Smith, C. L.; Cantor, C. R. *Nucleic Acids Res.* **1994**, *22*, 5530–5539.
(44) Huang, W. M.; Lehman, I. R. *J. Biol. Chem.* **1972**, *247*, 3139–3146.
(45) Green, S. J.; Lubrich, D.; Turberfield, A. J. *Biophys. J.* **2006**, *91*, 2966–2975.
(46) Turberfield, A. J.; Mitchell, J. C.; Yurke, B.; Mills, A. P., Jr.; Blakey, M. I.; Simmel, F. C. *Phys. Rev. Lett.* **2003**, *90*, 118102.
(47) Neeli, R.; Roitel, O.; Scrutton, N. S.; Munro, A. W. *J. Biol. Chem.* **2005**, *280*, 17634–17644.
(48) Shruti, K.; Shrey, K.; Vibha, R. *Biochem. Biophys. Res. Commun.* **2011**, *407*, 445–449.